

# On the Feeding Mechanisms for Graphene-based THz Plasmonic Nano-antennas

Josep Miquel Jornet

Department of Electrical Engineering  
University at Buffalo, The State University of New York  
Buffalo, New York 14260, USA  
E-mail: jmjornet@buffalo.edu

Albert Cabellos

NaNoNetworking Center in Catalonia (N3Cat)  
Universitat Politècnica de Catalunya, Barcelona, Spain  
E-mail: acabello@ac.upc.edu

**Abstract**—Graphene, thanks to its ability to support Surface Plasmon Polariton (SPP) waves in the Terahertz (THz) band (0.1-10 THz), enables the miniaturization and electrical tunability of miniature antennas suited for wireless communication among nanosystems. Despite graphene antennas have been extensively analyzed by means of modeling and simulation, no experimental proof is available to date. One of the main reasons for this is the lack of adequate signal generators and feeding mechanisms able to contact the nano-antenna with a reasonable efficiency. In this paper, two recently proposed feeding mechanisms for graphene-based THz plasmonic antennas are described. The first technique is based on the optical excitation of SPP waves by means of optical downconversion with photoconductive materials, whereas the second approach relies on electrical excitation of SPP waves on the antenna by means of a high-electron-mobility transistor. While fundamentally different, the two feeding mechanisms are able to effectively couple to a graphene-based plasmonic nano-structure and, thus, can be utilized to excite plasmonic nano-antennas in practical setups.

**Index Terms**—Graphene, plasmonics, nano-antenna, Terahertz-band communications

## I. INTRODUCTION

Throughout the last decades, wired and wireless communications have been enabled among devices with very diverse capabilities and dimensions, ranging from mainframes, desktop and laptop computers to home consumer electronics, mobile phones and sensors. Along with the continuous shrinking in the size of the devices, engineers have developed efficient communication means tailored to the peculiarities of each type of device. The resulting communication networks have enormously expanded the applications of the individual machines by providing them with a mechanism to cooperate.

Nowadays, nanotechnology is providing a new set of tools to design and manufacture miniaturized components such as physical, chemical and biological nanosensors [1]. Such devices require wireless communications for information sharing and coordination purposes, and this motivates the downscaling of transceivers and antennas. Unfortunately, reducing the size of a classical metallic antenna down to just a few micrometers would impose the use of very high resonant frequencies, from

the near infrared to the visible optical spectrum (hundreds of THz). At these frequencies, metals no longer behave as perfect electrical conductors [2], but exhibit a complex frequency-dependent conductivity that results in the propagation of confined electromagnetic (EM) waves, which are commonly referred to as Surface Plasmon Polariton (SPP) waves [3]. While the design of optical nano-antennas is a promising field, the use of optical signals would drastically limit the communication distance of individual nanosystems.

Alternatively, graphene has been shown to support SPP waves in the THz band (0.1-10 THz), i.e., at much lower frequencies than common metals [4]. This unique property has been leveraged to develop plasmonic nano-antennas or *graphennas*, with lateral dimensions of just a few micrometers or even less [5]. Compared to their metallic counterparts, graphennas resonate at a frequency almost two orders of magnitude lower [6]. In consequence, graphene antennas are envisaged to enable miniaturized wireless communications, and provide better integrability in future nanosystems.

Although graphene plasmons have been experimentally demonstrated down to the terahertz range [7], graphene antennas have been extensively analyzed by means of modeling and simulation only, and no experimental proof is available to date. One of the main challenges in the experimental demonstration of a graphene antenna is that, because of its typical resonant frequency, the antenna must be fed with a suitable THz source that can contact it with a reasonable efficiency. Ultimately, such source also needs to be integrated with the antenna to enable wireless communication among nano-systems.

In this paper, we describe two recently proposed feeding mechanisms for graphene-based THz plasmonic nano-antennas. On the one hand, in Sec. II, we present and analyze the performance of a feeding mechanism based on optical downconversion. In this setup, the graphene nano-antenna is fed with a photoconductive source, which is excited on its turn by an optical laser operated in pulsed mode [8]. On the other hand, in Sec. III, we describe the behavior of a solid-state electrical excitation mechanism for plasmonic nano-antennas, which is based on a hybrid High-Electron-Mobility Transistor (HEMT) built with a III-V semiconductor material enhanced

This work has been partially funded by Generalitat de Catalunya under grant 2014SGR-1427.

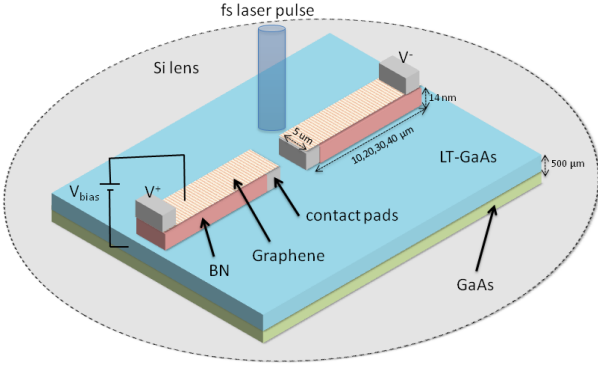


Fig. 1. Schematic representation of a graphene-based THz plasmonic antenna fed with a photoconductive material. The silicon lens aims to improve directivity.

with graphene [9]. Finally, we conclude the paper in Sec. IV.

## II. PHOTOCONDUCTIVE SOURCES FOR OPTICAL EXCITATION OF GRAPHENE-BASED NANO-ANTENNAS

The first proposed feeding mechanism for graphene-based THz plasmonic antennas is based on using a photoconductive source [10], [11]. The proposed setup, shown in Fig. 1, operates as follows: when a femtosecond laser pulse excites the biased semiconductor (e.g., Gallium Arsenide or GaAs) with a photon energy greater than its bandgap, electrons and holes are produced at the illumination point in the conduction and valence bands, respectively. The rapid change of the density of the photocarriers and their acceleration in the applied DC bias excites a time-varying current and an SPP wave at the interface between the graphene layer and the dielectric material. This time-varying excitation propagates along the graphene micro-antenna producing a free-space terahertz radiation. Finally, the silicon lens shown in Fig. 1 is a common technique used to improve the directivity of the radiated signal [12].

In order to characterize the proposed setup, we first model the time-dependent current density generated by the photoconductive source, based on a Drude-Lorentz model [10]. With this model, the time-dependent voltage at the antenna terminals  $V$  can be expressed as:

$$V(t) = Z_a \cdot j(t)\beta \cdot V_c(t), \quad (1)$$

where  $Z_a$  is the impedance of the graphene antenna,  $V_c$  is the voltage at the antenna gap, which is derived from its equivalent circuit [13],  $j(t)$  is the generated photocurrent density and  $\beta$  is the active area in the semiconductor through which the photocurrent flows.

In order to model the antenna, we use a full-wave EM solver as described in [6]. The radiation properties of graphene-based THz plasmonic antennas are mainly determined by the highly frequency-dependent behavior of the graphene electrical conductivity. In our analysis, we consider a surface conductivity model for infinitely-large graphene sheets, obtained using the

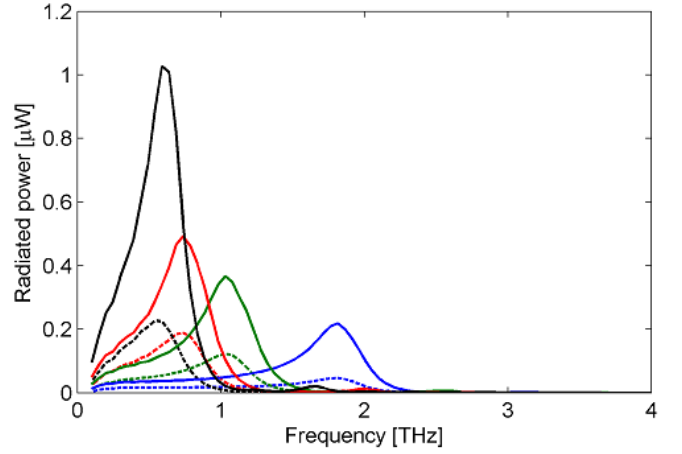


Fig. 2. Radiated power as a function of frequency for graphene antennas with lengths  $L = 10 \mu\text{m}$  (blue),  $20 \mu\text{m}$  (green),  $30 \mu\text{m}$  (red) and  $40 \mu\text{m}$  (black), from right to left, fed by a photoconductive source. The electron mobilities are  $\mu_g = 20,000 \text{ cm}^2/\text{V/s}$  (solid lines) and  $\mu_g = 10,000 \text{ cm}^2/\text{V/s}$  (dashed lines). The average optical power of the excitation laser is equal to 2 mW.

Kubo formalism [14], [15], and given by

$$\sigma^g = \sigma_{intra}^g + \sigma_{inter}^g, \quad (2)$$

$$\sigma_{intra}^g = \frac{2e^2 k_B T}{\pi \hbar} \frac{1}{\hbar} \ln \left( 2 \cosh \left( \frac{E_F}{2k_B T} \right) \right) \frac{i}{\omega + i\tau_g^{-1}}, \quad (3)$$

$$\sigma_{inter}^g = \frac{e^2}{4\hbar} \left( H \left( \frac{\omega}{2} \right) + i \frac{4\omega}{\pi} \int_0^\infty \frac{H(\epsilon) - H(\omega/2)}{\omega^2 - 4\epsilon^2} d\epsilon \right), \quad (4)$$

$$H(a) = \frac{\sinh(\hbar a/k_B T)}{\cosh(E_F/k_B T) + \cosh(\hbar a/k_B T)}, \quad (5)$$

where  $\omega = 2\pi f$ ,  $\hbar = h/2\pi$  is the normalized Planck's constant,  $e$  is the electron charge,  $k_B$  is the Boltzmann constant,  $T$  stands for temperature,  $E_F$  refers to the Fermi energy of the graphene sheet and  $\tau_g$  is the relaxation time of electrons in graphene, which depends on the electron mobility in graphene  $\mu_g$ .  $E_F$  can be easily modified by means of electrostatic bias,  $V_{bias}$  in Fig. 1, enabling tunable graphene antennas.

By combining the model for the photoconductive source with the graphene-based antenna, the radiated power is obtained. Fig. 2 shows the radiated power as a function of frequency for graphene antennas with lengths  $L=10 \mu\text{m}$  (blue),  $20 \mu\text{m}$  (green),  $30 \mu\text{m}$  (red) and  $40 \mu\text{m}$  (black), from right to left, fed by a photoconductive source. The assumed electron mobilities are  $20,000 \text{ cm}^2/\text{V/s}$  (solid lines) and  $10,000 \text{ cm}^2/\text{V/s}$  (dashed lines). The results, despite the high impedance present in graphene antennas and low radiation efficiency, the radiated power is in the same order of magnitude than traditional metallic photoconductive antennas. The main reason is that photoconductive sources have also typically a very high impedance, and this allows to operate closer to impedance matching, compensating the low radiation efficiency. We refer the interested reader to [8] for more details about the model, simulation and results.

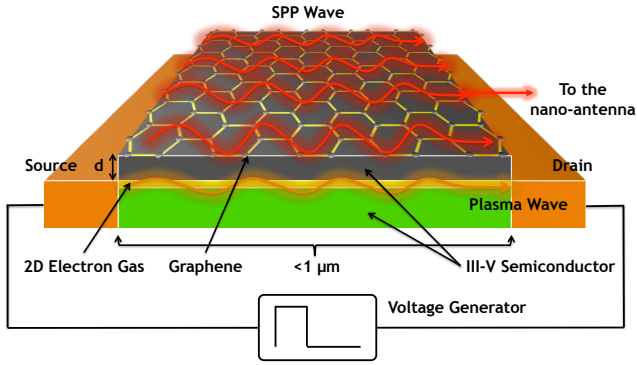


Fig. 3. Hybrid graphene/semiconductor HEMT-based THz signal source.

### III. HYBRID HIGH-ELECTRON-MOBILITY TRANSISTOR FOR ELECTRICAL EXCITATION OF GRAPHENE-BASED NANO-ANTENNAS

Also, it has been recently proposed a feeding mechanism based on a novel graphene-based plasmonic nano-transmitter able to generate SPP waves at THz frequencies [9].

Our electrically-injected plasmonic source, which is shown in Fig. 3, consists of a HEMT built with a III-V semiconductor and a graphene-layer at the gate [16]. When a positive voltage is applied between the drain and the source of the HEMT, electrons are accelerated from the source to the drain. As first described in [17] and experimentally shown in several works [18], electrons moving in the HEMT channel create a plasma wave through the Dyakonov-Shur instability. For a channel length in the order of a hundred nanometers, the plasma wave in the 2D electron gas (2DEG) resonates in the THz band. Contrary to existing THz band sources, in our proposed design, the plasma wave is not directly radiated, but used to induce a propagating SPP wave at the interface with the graphene layer. The oscillating image charge created at the graphene-semiconductor interface in response to the confined plasma wave oscillation results in a coupled oscillating charge distribution at or near the frequency at which the system is driven [19]. Due to the complex conductivity of graphene at THz band frequencies, given by (2), this global oscillation of charge in the graphene-semiconductor interface results in an SPP wave, which propagates to the nano-antenna.

To analyze the performance of this THz signal source, first, we need to model the excitation of the plasma wave in the HEMT channel. A DC current must flow in the HEMT channel to initiate the Dyakonov-Shur instability, which should develop when asymmetric boundary conditions are realized at opposite ends of the channel. In particular, source terminal needs to exhibit a near-short-circuit for the plasma excitation, i.e., it needs to be grounded, whereas a near-open-circuit condition needs to be realized close to the drain. Under these conditions, the HEMT channel behaves as a plasmonic cavity. Then, the dispersion equation for a 2D plasma wave in 2DEG of the

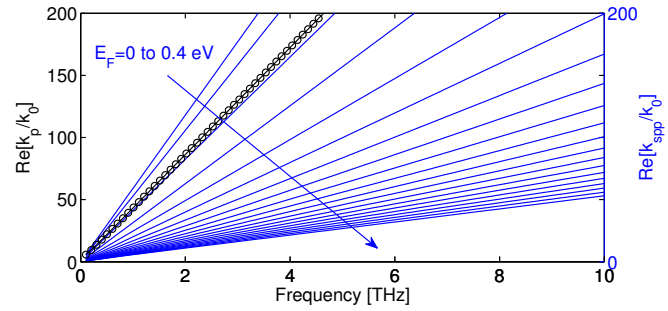


Fig. 4. Wavevector for 2D plasmons in the HEMT channel and wavevectors for 2D SPP waves in graphene.

HEMT channel is given by [20]:

$$\frac{\varepsilon_r^{(1)}}{\sqrt{k_p^2 - \frac{\varepsilon_r^{(1)}\omega^2}{c_0^2}}} + \frac{\varepsilon_r^{(2)}}{\sqrt{k_p^2 - \frac{\varepsilon_r^{(2)}\omega^2}{c_0^2}}} = -i\frac{\sigma^{sc}}{\omega\varepsilon_0}, \quad (6)$$

where  $k_p$  is the plasmon wavevector and the conductivity of the semiconductor material  $\sigma^{sc}$  is given by

$$\sigma^{sc} = \frac{e^2 n_s^{sc} \tau^{sc}}{(1 - i\omega\tau^{sc}) m^{*sc}}, \quad (7)$$

where  $n_s^{sc}$  is the 2D electron density,  $\tau^{sc}$  is the 2D relaxation time, and  $m^{*sc}$  is the 2D electron effective mass in the semiconductor. The 2D electron density can be approximated by

$$n_s^{sc} = C \frac{U}{e} = \frac{\varepsilon_0 \varepsilon_r U}{d e}, \quad (8)$$

where  $C$  is the gate capacitance per unit area,  $U$  is the gate-to-channel voltage and  $d$  is the gate insulator thickness.

Second, we need to analyze the mechanism by which the 2D plasmon in the HEMT channel can launch an SPP wave on graphene. 2D plasmons in the HEMT channel can couple to plasmons in the graphene layer by means of the Coulomb interaction. Coupling is achieved when the wavevectors of both plasmons are closely matched. The wavevector for an SPP wave on graphene can be obtained by solving (6), with  $k_{spp}$  instead of  $k_p$  and conductivity  $\sigma^g$  given by (2), instead of  $\sigma^{sc}$ .

In Fig. 4, we plot the dispersion curve (6) for both 2D plasmons in the HEMT channel as well as SPP waves on graphene for different values of the Fermi energy. In our analysis, we consider that GaAs is used in the HEMT, with  $\varepsilon_r=13.1$ ,  $m^{*sc} = 0.067m_e$ , drift velocity,  $v_0 = 2 \cdot 10^5$  m/s and thickness,  $d = 50$  nm. For graphene, we consider  $\mu^g = 1$  m<sup>2</sup>/V/s and  $v_F=c/300$ . The results clearly demonstrate that matching can be achieved over a broad range of THz frequencies, for wavevectors corresponding to plasmonic cavities of sub-micron size. This proves the feasibility of the proposed approach and motivates its further analysis.

### IV. CONCLUSIONS

In this paper, we have presented two alternatives to excite graphene-based plasmonic THz nano-antennas. The first

technique is based on optical pumping of a photoconductive antenna attached to the graphene structure. This technique has basically two main advantages. First, such terahertz sources have typically a very high impedance, in the order of several  $k\Omega$ , which lies in the same order of magnitude of the input impedance of graphene antennas [21], thereby improving impedance matching between both devices. Second, ultrafast photoconductive antennas operate in pulsed mode, which is also the proposed fundamental mechanism for EM communications among nanosystems [22]. The second alternative is based on the electrical generation of a plasma wave in the channel of a HEMT by means of the Dyakonov-Shur instability and its coupling to a SPP wave on graphene. In this case, it has been shown that the impedance match problem with the graphene antenna is overcome by wireless coupling to it. In addition, the very small size of the signal source allows it to be embedded on chip with the nano-system. While fundamentally different, the two feeding mechanisms are able to effectively couple to a graphene-based plasmonic nanostructure and, thus, can be utilized to excite plasmonic nanoantennas in practical setups.

#### REFERENCES

- [1] I. F. Akyildiz and J. M. Jornet, "Electromagnetic wireless nanosensor networks," *Nano Communication Networks (Elsevier) Journal*, vol. 1, no. 1, pp. 3–19, Mar. 2010.
- [2] P. R. West, S. Ishii, G. V. Naik, N. K. Emani, V. M. Shalaev, and A. Boltasseva, "Searching for better plasmonic materials," *Laser & Photonics Reviews*, vol. 4, no. 6, pp. 795–808, 2010.
- [3] Q.-H. Park, "Optical antennas and plasmonics," *Contemporary physics*, vol. 50, no. 2, pp. 407–423, 2009.
- [4] J. Horng, C.-F. Chen, B. Geng, C. Girit, Y. Zhang, Z. Hao, H. A. Bechtel, M. martin, A. Zettl, M. F. Crommie, Y. R. Shen, and F. Wang, "Drude conductivity of dirac fermions in graphene," *Physical Review B*, vol. 83, p. 165113, Apr. 2011.
- [5] J. M. Jornet and I. F. Akyildiz, "Graphene-based plasmonic nano-antenna for terahertz band communication in nanonetworks," *IEEE JSAC, Special Issue on Emerging Technologies for Communications*, vol. 12, no. 12, pp. 685–694, Dec. 2013.
- [6] I. Llatser, C. Kremers, A. Cabellos-Aparicio, J. M. Jornet, E. Alarcon, and D. N. Chigrin, "Graphene-based nano-patch antenna for terahertz radiation," *Photonics and Nanostructures - Fundamentals and Applications*, vol. 10, no. 4, pp. 353–358, Oct. 2012.
- [7] L. Ju, B. Geng, J. Horng, C. Girit, M. martin, Z. Hao, H. Bechtel, X. Liang, A. Zettl, Y. R. Shen, and F. Wang, "Graphene plasmonics for tunable terahertz metamaterials," *Nature Nanotechnology*, vol. 6, pp. 630–634, Sep. 2011.
- [8] A. Cabellos-Aparicio, I. Llatser, E. Alarcon, A. Hsu, and T. Palacios, "Use of thz photoconductive sources to characterize tunable graphene rf plasmonic antennas," *IEEE Transactions on Nanotechnology*, vol. -, no. -, pp. -, 2015.
- [9] J. M. Jornet and I. F. Akyildiz, "Graphene-based plasmonic nano-transceiver for terahertz band communication," in *Proc. of European Conference on Antennas and Propagation (EuCAP)*, 2014.
- [10] D. Auston, K. Cheung, and P. Smith, "Picosecond photoconducting hertzian dipoles," *Applied physics letters*, vol. 45, no. 3, pp. 284–286, 1984.
- [11] C. Berry, N. Wang, M. Hashemi, M. Unlu, and M. Jarrahi, "Significant performance enhancement in photoconductive terahertz optoelectronics by incorporating plasmonic contact electrodes," *Nature communications*, vol. 4, p. 1622, 2013.
- [12] M. Tani, S. Matsuura, K. Sakai, and S.-i. Nakashima, "Emission characteristics of photoconductive antennas based on low-temperature-grown gaas and semi-insulating gaas," *Applied optics*, vol. 36, no. 30, pp. 7853–7859, 1997.
- [13] N. Khiabani, Y. Huang, Y.-C. Shen, and S. Boyes, "Theoretical modeling of a photoconductive antenna in a terahertz pulsed system," *IEEE transactions on antennas and propagation*, vol. 61, no. 4, pp. 1538–1546, 2013.
- [14] L. Falkovsky and A. A. Varlamov, "Space-time dispersion of graphene conductivity," *The European Physical Journal B*, vol. 56, pp. 281–284, 2007.
- [15] G. W. Hanson, "Dyadic Green's functions and guided surface waves for a surface conductivity model of graphene," *Journal of Applied Physics*, vol. 103, no. 6, p. 064302, 2008.
- [16] J. K. Park, S. M. Song, J. H. Mun, and B. J. Cho, "Graphene gate electrode for mos structure-based electronic devices," *Nano letters*, vol. 11, no. 12, pp. 5383–5386, 2011.
- [17] M. Dyakonov and M. Shur, "Shallow water analogy for a ballistic field effect transistor: New mechanism of plasma wave generation by dc current," *Phys. Rev. Lett.*, vol. 71, pp. 2465–2468, Oct 1993.
- [18] T. Otsuji, T. Watanabe, S. Boubanga Tombet, A. Satou, W. Knap, V. Popov, M. Ryzhii, and V. Ryzhii, "Emission and detection of terahertz radiation using two-dimensional electrons in iii-v semiconductors and graphene," *IEEE Transactions on Terahertz Science and Technology*, vol. 3, no. 1, pp. 63–71, 2013.
- [19] P. Xu, S. D. Barber, M. L. Ackerman, J. Kevin Schoelz, and P. M. Thibado, "Role of bias voltage and tunneling current in the perpendicular displacements of freestanding graphene via scanning tunneling microscopy," *Journal of Vacuum Science & Technology B: Microelectronics and Nanometer Structures*, vol. 31, no. 4, pp. 04D103–04D103, 2013.
- [20] F. Stern, "Polarizability of a two-dimensional electron gas," *Physical Review Letters*, vol. 18, pp. 546–548, Apr. 1967.
- [21] M. Tamagnone, J. Gomez-Diaz, J. Mosig, and J. Perruisseau-Carrier, "Analysis and design of terahertz antennas based on plasmonic resonant graphene sheets," *Journal of Applied Physics*, vol. 112, no. 11, p. 114915, 2012.
- [22] J. M. Jornet and I. F. Akyildiz, "Femtosecond-long pulse-based modulation for terahertz band communication in nanonetworks," *IEEE Transactions on Communications*, vol. 62, no. 5, pp. 1742 – 1754, May 2014.